MTOpen

original article

Systemic Gene Delivery in Large Species for Targeting Spinal Cord, Brain, and Peripheral Tissues for Pediatric Disorders

Adam K Bevan[1,2], Sandra Duque[3], Kevin D Foust[1], Pablo R Morales[4], Lyndsey Braun[1], Leah Schmelzer[1], Curtis M Chan[5], Mary McCrate[1,6], Louis G Chicoine[1,6], Brian D Coley[7], Paul N Porensky[3,8], Stephen J Kolb[3,9], Jerry R Mendell[1,6,9], Arthur HM Burghes[2,3] and Brian K Kaspar[1–3,6,10]

[1]Center for Gene Therapy, The Research Institute at Nationwide Children's Hospital, Columbus, Ohio, USA; [2]Integrated Biomedical Sciences Graduate Program, The Ohio State University, Columbus, Ohio, USA; [3]Department of Molecular and Cellular Biochemistry, The Ohio State University, Columbus, Ohio, USA; [4]The Mannheimer Foundation, Inc., Homestead, Florida, USA; [5]Special Pathology Services, Charles River, Preclinical Services, Reno, Nevada, USA; [6]Department of Pediatrics, The Ohio State University/Nationwide Children's Hospital, Columbus, Ohio, USA; [7]Department of Radiology, The Ohio State University, Columbus, Ohio, USA; [8]Department of Neurological Surgery, The Ohio State University, Columbus, Ohio, USA; [9]Department of Neurology, The Ohio State University, Columbus, Ohio, USA; [10]Department of Neurosciences, The Ohio State University, Columbus, Ohio, USA

Adeno-associated virus type 9 (AAV9) is a powerful tool for delivering genes throughout the central nervous system (CNS) following intravenous injection. Preclinical results in pediatric models of spinal muscular atrophy (SMA) and lysosomal storage disorders provide a compelling case for advancing AAV9 to the clinic. An important translational step is to demonstrate efficient CNS targeting in large animals at various ages. In the present study, we tested systemically injected AAV9 in cynomolgus macaques, administered at birth through 3 years of age for targeting CNS and peripheral tissues. We show that AAV9 was efficient at crossing the blood–brain barrier (BBB) at all time points investigated. Transgene expression was detected primarily in glial cells throughout the brain, dorsal root ganglia neurons and motor neurons within the spinal cord, providing confidence for translation to SMA patients. Systemic injection also efficiently targeted skeletal muscle and peripheral organs. To specifically target the CNS, we explored AAV9 delivery to cerebrospinal fluid (CSF). CSF injection efficiently targeted motor neurons, and restricted gene expression to the CNS, providing an alternate delivery route and potentially lower manufacturing requirements for older, larger patients. Our findings support the use of AAV9 for gene transfer to the CNS for disorders in pediatric populations.

Received 8 June 2011; accepted 5 July 2011; published online 2 August 2011. doi:10.1038/mt.2011.157

INTRODUCTION

The recent discovery that adeno-associated virus type 9 (AAV9) can cross the blood–brain barrier (BBB) and produce extensive transgene expression in the brain and spinal cord suggests a powerful, noninvasive method to deliver genes to the central nervous system (CNS). Preclinical results in models of pediatric neurological diseases with widespread pathology indicate systemic gene delivery could have profound therapeutic benefits, such as in spinal muscular atrophy (SMA). SMA is the most common autosomal recessive disease of early childhood with an incidence of 1:6–10,000 live births. In its most common and severe form (type 1), hypotonia and progressive weakness are recognized in the first few months of life, leading to diagnosis by 6 months of age and death due to respiratory failure by age two.[1] There is no treatment available to slow or halt disease progression, but recent preclinical studies utilizing gene delivery in newborn rodent models of SMA suggest gene therapy may hold promise.[2–4] SMA is an attractive disease for gene therapy because it is a single gene defect that most frequently results in low amounts of the survival motor neuron (SMN) protein versus a total deficiency.[1] SMN is a ubiquitously expressed protein that is essential in all tissues and is not associated with toxicity when over expressed.[2–8] In addition, disease severity correlates with SMN protein levels suggesting that increasing SMN may be beneficial for patients.[6] Motor neurons are the cell type primarily responsible for pathology of SMA, which has precluded the development of an SMA gene therapy due to inefficient targeting of these cells by recombinant vectors.[9] However, the recent discovery that AAV9 can target ~60% of motor neurons after systemic injection makes efficient delivery to the CNS feasible.[10,11]

A critical step in the translation of an SMA therapy to clinic is the demonstration of CNS targeting in nonhuman primates. AAV9's crossing of the BBB has been demonstrated in mice, rats, and cats indicating promise for translation to a human population.[10–13] Importantly, we demonstrated that AAV9 can target motor neurons following intravenous injection in a 1-day-old cynomolgus macaque.[3] However, the data in mice suggests a window of opportunity for targeting motor neurons in young

The first three authors contributed equally to this work.

Correspondence: *Brian K Kaspar, Center for Gene Therapy, The Research Institute at Nationwide Children's Hospital, 700 Children's Dr, Room WA3022, Columbus, Ohio 43205; Phone: 614-722-2700, Fax: 614-355-5247; E-mail: brian.kaspar@nationwidechildrens.org*

primates may remain as a potential clinical obstacle for advancing AAV9 gene delivery for SMA. When AAV9 is systemically administered to newborn mice, there is extensive neuronal transduction throughout the brain and spinal cord. However, when administered to adult mice, the majority of transduced cells are positive for astrocytic markers.[11] Our studies in mice demonstrated that this "switch" in targeted cell types occurred within the first 10 days of life as demonstrated by a progressive decline in motor neuron transduction between P2 and P10.[3]

For this reason, we examined transgene expression throughout the body of male cynomolgus macaques following vascular delivery at time points from birth through 3 years of age using self-complementary AAV9 delivery of green fluorescent protein (GFP) versus phosphate-buffered saline (PBS) controls. In the present work, we expand our earlier findings that systemically administered AAV9 can efficiently target motor neurons in a newborn nonhuman primate with the addition of successful motor neuron targeting in animals up to 3 years of age. We also demonstrate extensive transduction of primarily glial cells throughout the brains of all treated animals. We extend our examination to tissues outside of the CNS and report extensive transgene expression within skeletal muscle and multiple organs. Because system-wide transduction may not be desirable in every paradigm, we investigated intrathecal and intracisternal delivery of AAV9 in newborn pigs for its ability to produce CNS transduction.[14] We demonstrate that motor neurons and regions of the brain can be targeted in neonatal pigs using AAV9 delivery to cerebrospinal fluid (CSF), potentially increasing the specificity and lowering the viral dose required for efficacy.[15] Together these findings are supportive of advancing AAV9-based gene delivery to the clinic for treatment of newly diagnosed type 1 SMA patients. In addition to SMA, the extensive transduction seen in the brain at all time points suggests applications for other pediatric neurological diseases with global pathology such as Rett syndrome and lysosomal storage disorders.

RESULTS

Systemic injection of AAV9 targets motor neurons in nonhuman primates through 3 months

The observation that, in mice, the cell types targeted by systemic injection of AAV9 shifted from neurons to astrocytes early in postnatal life could impact the potential clinical utility of AAV9. To address whether this pattern was unique to rodents, we sought to define a window of opportunity for targeting motor neurons in nonhuman primates following systemic delivery of AAV9-GFP. We performed systemic injections of $1–3 \times 10^{14}$ vg/kg in a maximum volume of 10 ml of self-complementary AAV9-GFP with a chicken β-actin hybrid promoter, a cytomegalovirus immediate early enhancer and an SV40 intron. This is the same promoter construct previously used in our initial AAV9 report as well as in our rescue of the SMA mouse model report.[3,11] With the exception of P1 animals, serum samples from male cynomolgus macaques were screened for the presence of binding antibodies against AAV9 capsids using an anti-AAV9 enzyme-linked immunosorbent assay. Animals that were seronegative at 1:50 (the lowest dilution tested) for anti-AAV9 antibodies were injected through the saphenous vein at postnatal day 1, 30, or 90 (P1, P30, or P90, respectively). Animals were killed 21–25 days postinjection and tissues collected for analysis. We performed *in situ* hybridization on lumbar spinal cord sections of the AAV9 GFP- and PBS-injected monkeys. Use of an antisense probe against the GFP mRNA detected abundant signal (**Figure 1a,c,e**; dark blue dots) that colocalized with a nuclear counter stain (pink) in the vector-treated animals. GFP expression was seen in large neurons of the ventral horn and within small nuclei throughout the gray and white matter of all the AAV-treated monkeys. Nearly all of the large neuronal-like cells displayed detectable levels of positive signal with additional cells targeted throughout the spinal cord, which likely demonstrates non-neuronal transduction. PBS-treated animals had no detectable signal in any of the sections examined (**Figure 1g**). To confirm that the signal was not the result of nonspecific binding of the antisense probe, tissue sections from the same animals were exposed to a sense probe which does not bind mRNA. Importantly, there was no hybridization in sections from either vector or PBS-treated animals when using the sense probe (**Figure 1b,d,f,h**).

To identify the GFP^+ neurons in the spinal cord, we immunolabeled tissue sections for transgene and choline acetyl transferase (ChAT), a motor neuron marker. Examination of labeled sections at all levels of the spinal cord demonstrated extensive GFP labeling in $ChAT^+$ cells in all of the treated monkeys (P1–P90) (**Figure 2**).

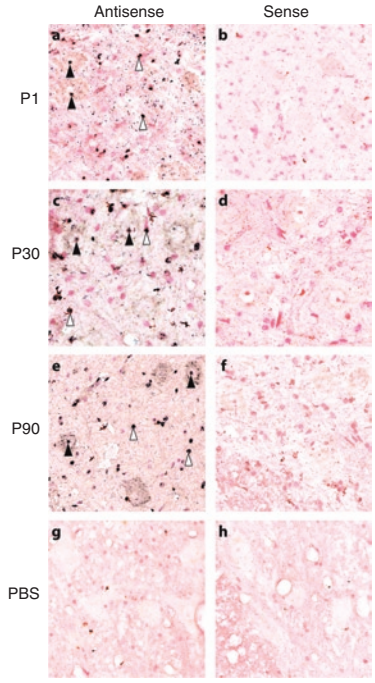

Figure 1 ***In situ*** **hybridization of monkey spinal cords following intravenous injection of either adeno-associated virus type 9 (AAV9)-green fluorescent protein (GFP) or phosphate-buffered saline (PBS).** Regions of lumbar spinal cords were probed with either antisense (**a**,**c**,**e**, and **g**) or sense (**b**,**d**,**f**, and **h**) probes against the vector-derived GFP mRNA then counterstained with fast-red as a nuclear label. Within sections incubated with antisense probe, positive labeling is shown in dark blue, and is detected in large ventral neurons (filled arrows) and glia (open arrows) throughout both the gray and white matter of all animals injected with AAV9-GFP. There was no detectable signal when vector-treated tissues were incubated with the sense probe indicating a lack of nonspecific probe binding. PBS-treated animals had no detectable signal with either the antisense or sense probes.

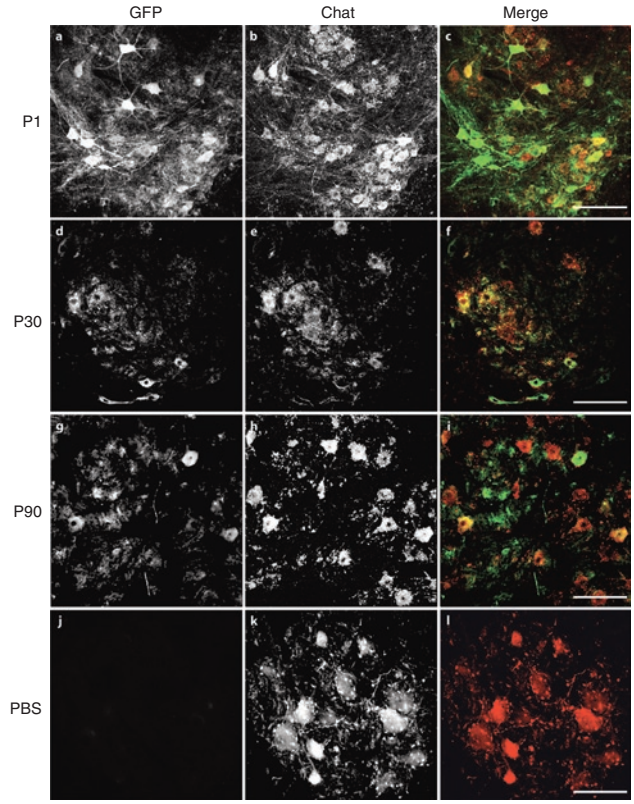

Figure 2 Immunofluorescent labeling of green fluorescent protein (GFP) and choline acetyl transferase (ChAT) within motor neurons. Lumbar spinal cord sections from adeno-associated virus type 9 (AAV9) or phosphate-buffered saline (PBS)-injected animals were labeled with antibodies against the vector-derived transgene (GFP; **a**,**d**,**g**, and **j**) and a motor neuron marker (ChAT; **b**,**e**,**h**, and **k**) and are shown in black and white for enhanced contrast. Merged images (**c**,**f**,**i**, and **l**), GFP in green and ChAT in red, indicate extensive transgene expression within motor neurons of the P1, P30, and P90-injected animals. GFP expression was not detected within the spinal cords of PBS-injected animals. All Bars = 200 µm.

GFP$^+$ nerve fibers were also detected coursing through the dorsomedial white matter indicative of transgene expression within the ganglion cells of the dorsal root (**Supplementary Figure S1**). As seen with mice, GFP expression within neurons in the parenchyma of the spinal cord was confined to ChAT$^+$ cells. There was also GFP$^+$ cells with glial morphology that were sparsely scattered throughout the sections examined (data not shown). The overall pattern as detected by GFP immunohistochemistry was similar to that seen after neonatal delivery of AAV9 in rodents and cats with expression primarily in neuronal cells that project into the periphery.[10,11] Importantly, efficient motor neuron targeting with AAV9 persists through at least the first three postnatal months.

Intravascular delivery of AAV9 targets motor neurons in a 3-year-old cynomolgus macaque

Due to successful targeting of motor neurons through the first 3 months of life in nonhuman primates, we asked whether motor neurons could still be targeted in a 3-year-old cynomolgus macaque. Utilizing interventional radiological techniques, a catheter was threaded through the brachial artery to the descending aorta while a balloon catheter was simultaneously fed through the femoral artery to the celiac artery and transiently inflated during vector injection. A dose of 2.7×10^{13} vg/kg of AAV9-GFP was administered to the descending aorta while partially occluding blood flow to the liver in a procedure designed to give "first-pass" of the virus through the spinal arteries that are responsible for blood flow to the nerve roots of the thoracic cord. Two weeks postinjection; the animal was killed and examined for GFP expression using *in situ* hybridization and GFP immunofluorescence. As with the P1–P90 animals, antisense probed sections of spinal cord indicated GFP expression within both neuronal and glial cells of the spinal cord, while sense probed sections showed no signal (**Supplementary Figure S2a,b**). GFP and ChAT immunofluorescent examination of cervical, thoracic, and lumbar spinal cord sections revealed GFP$^+$ motor neurons at all levels though less frequently than in younger animals (**Supplementary Figure S2c,e**). The apparent decrease in motor neuron transduction may be due to 1/10 the dose given to the 3-year-old animal compared to that of the P1–P90 group. Nevertheless, this is the proof that motor neurons can still be targeted utilizing systemic AAV9 delivery in a juvenile cynomolgus macaque even at significantly lower doses.

Intravascular AAV9 produces extensive glial transduction throughout the brain

We next examined brain transduction following systemic delivery of AAV9. Indeed in mice, intravenous injection of AAV9 produced high levels of neuronal transduction in the brain, therefore, we examined the brains of the treated monkeys for GFP expression utilizing immunohistochemistry.[11] As performed with the spinal cords, whole mount brains were sectioned in a serial manner and evaluated for GFP expression. Representative sections using high resolution slide scanning are shown in **Figure 3** (P1–P90) and **Supplementary Figure S3** (3 years). Slide scanning technology captures images of the entire microscope slide with up to ×40 resolution.[16] All GFP-injected animals had extensive transgene expression throughout the entire brain. The overall pattern of expression was again similar to that seen in mice with the most abundant number of GFP-expressing cells in all cortical regions (**Figure 3a,b,f–j,k,o**), lateral geniculate (**Figure 3a,d**), midbrain, pons and medulla. Subcortical structures such as thalamus (**Figure 3a,c**) and putamen (**Figure 3k,l**) were also GFP$^+$ but at a lower cell density. In contrast to the mice, primate brains of all ages had primarily glial transduction with microglia and astrocytes being the most prominent cell types targeted (**Supplementary Figure S4**) as determined by colabeling with Iba-1 and GFAP (microglia and astrocyte marker, respectively) with neurons interspersed throughout. The scarcity of neuronal transduction was most striking in the hippocampus (**Figure 3k,n**) and dentate gyrus of the nonhuman primates because, in mice, neurons of these regions were highly transduced in both neonate- and adult-treated animals.[11] Transduction was not restricted to gray matter (**Figure 3k,m**) and included scattered oligodendrocytes (data not shown). Surprisingly, widespread GFP expression was seen throughout the brain of the 3-year-old animal that received 1/10 the dose compared to the P1–P90 animals. The brain regions transduced in the older animal were consistent with the younger primates

with cortical and pontine regions having the highest prevalence of transduced cells. GFP$^+$ cells were predominantly astrocytes and microglia (data not shown) though neurons of cranial nerve nuclei also expressed GFP (**Supplementary Figure S3b**).

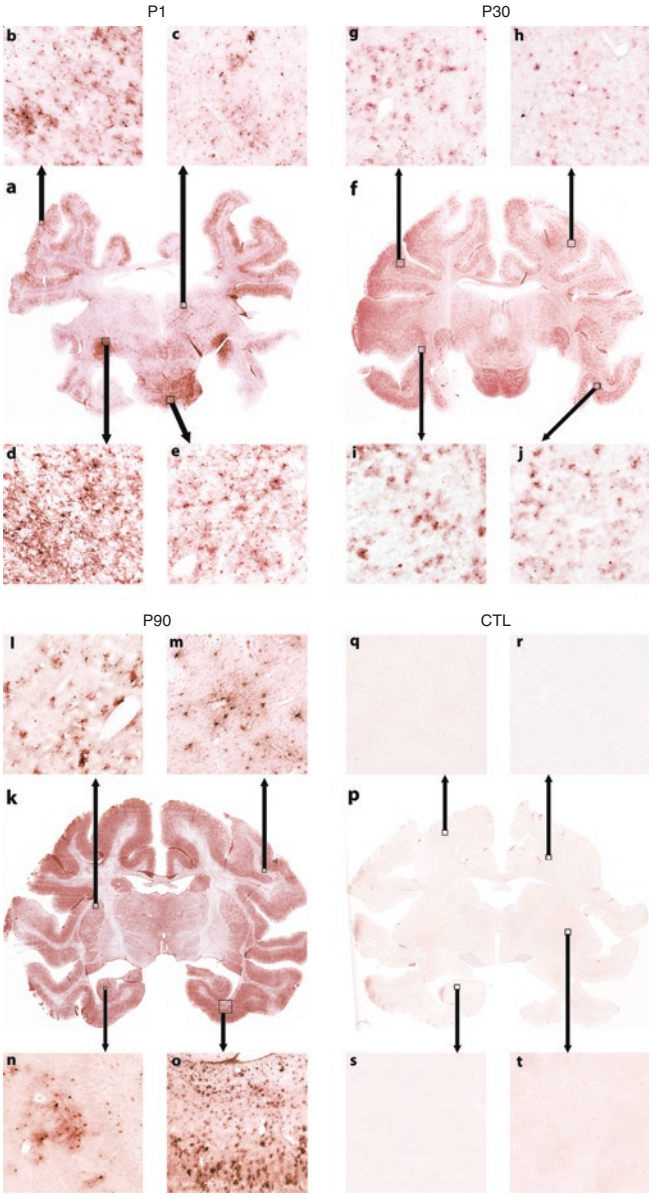

Figure 3 Whole slide scans of adeno-associated virus type 9 (AAV9) and phosphate-buffered saline (PBS)-injected monkey brains. Representative sections through similar regions of brains from systemically injected monkey were immunolabeled with anti-GFP antibodies. Panels **a**,**f**, and **k** show uniform labeling throughout the sections of AAV9-injected animals but not the (**p**) PBS-injected animals. Boxes and arrows indicate the approximate regions from where the high magnification images were acquired. Cortex (**a**,**b**,**f**–**j**,**k**, and **o**) consistently had the highest density of GFP-expressing cells at all time points as did the lateral geniculate (**a**,**d**). Subcortical structures such as thalamus (**a**,**c**) and putamen (**l**,**k**) were well transduced but at a lower density than cortex. GFP$^+$ cells were also seen within white matter of the pons (**a**,**f**,**e**) and cortex (**k**,**m**), as well as within the hippocampus (**k**,**n**). The majority of GFP$^+$ cells in all regions had glial morphology though individual neurons could be detected throughout the brain. Brains from PBS-injected animals were negative for GFP signal (**p**–**t**).

AAV9 transduces skeletal muscle and peripheral organs

Numerous groups have demonstrated the ability of AAV to efficiently target skeletal muscle in mice, dogs, and primates.[17–21] Therefore, we examined skeletal muscle of the AAV9-injected nonhuman primates for GFP expression. In the young monkeys (P1–P90), all skeletal muscles examined were positive for GFP using immunofluorescent detection (**Figure 4**) including triceps, diaphragm, transverse abdominus, quadriceps, gastrocnemius, tibialis anterior, and tongue. Skeletal muscles sampled were from the brachial and pelvic limbs, head, and trunk indicating a body-wide distribution. GFP expression was less abundant in the skeletal muscles of the lower dosed, older monkey though still detectable in most muscles (data not shown).

Peripheral organs may also be a target of a systemically injected vector, therefore, we collected organs from injected animals to look for GFP expression within tissues (**Figure 5**). Although,

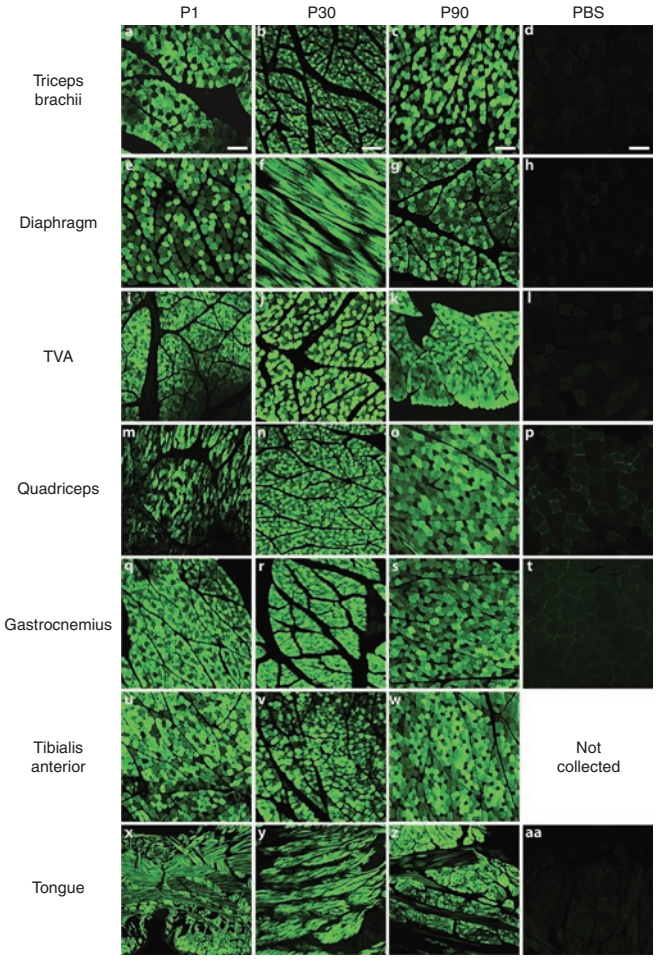

Figure 4 Green fluorescent protein (GFP) expression within nonhuman primate skeletal muscle. GFP immunofluorescence from adeno-associated virus type 9 (AAV9)-injected and phosphate-buffered saline (PBS)-injected monkeys demonstrates extensive transgene expression in skeletal muscles of all AAV9-injected animals. GFP expression was detected in the brachial limbs (triceps brachii **a**–**c**), trunk [diaphragm **e**–**g** and transverse abdominus (TVA) **i**–**k**], pelvic limbs (quadriceps **m**–**o**, gastrocnemius **q**–**s**, and tibialis anterior **u**–**w**) and head (tongue **x**–**z**) of AAV9 systemically injected animals. No GFP signal was detected in any of the muscle from the PBS-injected animals (**d**,**h**,**l**,**p**,**t**, and **aa**).

we could detect native GFP expression, we utilized an antibody against GFP to enhance detection levels. As expected, liver had the highest levels of GFP expression, followed by the adrenal medulla (P1-injected animal). Previous studies demonstrated that the heart, while well targeted in mice by AAV9, is not as efficiently transduced in dogs.[18,22] Our findings in the AAV9-treated monkeys agree with those in dog, in that levels of GFP expression in the heart were lower relative to skeletal muscle. GFP signal was also found in the germinal centers of the spleen in all of the treated animals as well as smooth muscle that lines the intestines. GFP expression was also detected in the Leydig cells of the testes of all treated male monkeys. Finally, occasional positive cells were identified in the lungs and kidneys of AAV9 GFP-treated animals.

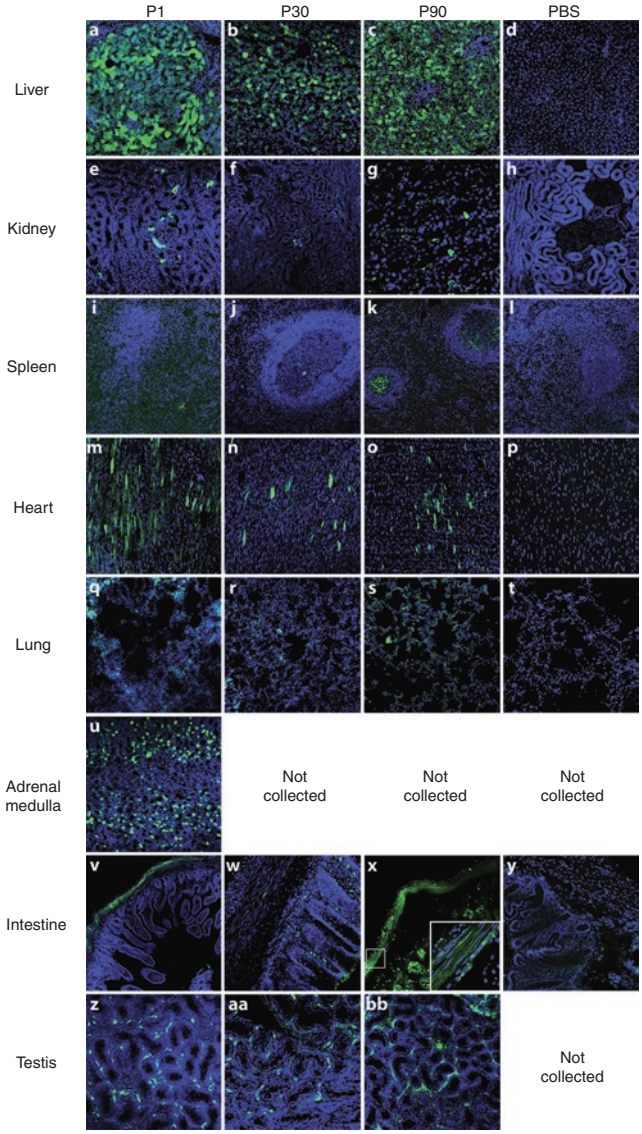

Figure 5 Green fluorescent protein (GFP) expression within assorted organs. Of the tissues examined, GFP expression was most abundant in the (**a**–**c**) livers and (**u**) adrenal medulla of all AAV9-injected monkeys. Detectable GFP expression was also seen in the (**e**–**g**) kidney, (**i**–**k**) spleen, (**m**–**o**) heart, (**q**–**s**) lung, (**v**–**x**) smooth muscle of the intestines, and(**z**–**bb**) testes of AAV-injected animals. GFP was not detected in the tissues collected from PBS-injected animals (**d**,**h**,**l**,**p**,**t**, and **y**).

These results demonstrate that systemic gene delivery targets multiple organ systems with a biodistribution of expression similar to that found in the rodent with the exception of cardiac tissue.

AAV9 injection into cerebral spinal fluid of young pigs efficiently targets motor neurons

Although some neurological disorders are caused by defects in ubiquitously expressed proteins, in other disorders gene expression in the CNS alone may have a substantial impact.[23–25] Gene delivery to the CSF could produce transduction along the neuraxis with the added benefit of potentially lowering the required dose. In order to examine more localized CNS delivery we performed intrathecal and/or intracisternal injections of 5.2×10^{12} vg/kg of AAV9 GFP into 5-day-old pigs ($n = 3$ each) and examined their brains and spinal cords for GFP expression. In all animals, GFP expression was seen in the dorsal root ganglia as well as the spinal cord gray and white matter. Importantly, AAV9 GFP injection into either the cisternal space at the base of the skull or the intrathecal space at L5 resulted in extensive motor neuron transduction at all levels of the spinal cord (**Figure 6a–d**) as examined by *in situ* hybridization. Large ventral horn neurons were also positive for GFP expression by immunohistochemistry at all levels of spinal cord (**Figure 6e–l**). Immunofluorescence confirmed that the GFP^+ cells expressed the motor neuron marker ChAT (**Figure 6m–r**).

AAV9 injection into the CSF produces transgene expression in the brain

Finally, to further characterize the pattern of expression following cisternal or intrathecal injection of AAV9-GFP into 5-day-old pigs, we examined brains for transgene expression again using GFP immunofluorescence (**Figure 7**). The regions with the highest levels of GFP expression were cerebellar Purkinje cells, nerve fibers within the medulla as well as discrete nuclei, such as the olivary nucleus. Expression within the rest of the brain was restricted to scattered cells near the meningeal surfaces (data not shown). Examination of GFP expression in peripheral organs yielded no visible GFP expression indicating that the majority of the virus was localized to the CNS.

DISCUSSION

The recent emergence of AAV9 and its ability to cross the BBB represents a potentially valuable therapeutic and basic science tool. The consistency of performance across species only adds to AAV9's value. Our previous work and the data presented here are among the first to demonstrate transgene expression within the entire CNS following a peripheral systemic injection in nonhuman primates.[3,12] That a similar pattern of expression is generated in animals of multiple ages is excellent proof-of-concept that this delivery modality can be advanced to the clinic, especially for pediatric diseases with broad targeting needs.

A recent study also looked at systemic injection of AAV9 for its ability to cross the BBB in nonhuman primates.[12] Both the present and previous studies report transgene expression along the entire neuraxis of nonhuman primates. What is further encouraging about the two data sets is that Gray *et al.* worked exclusively in 3–4-year-old male rhesus macaques at 1/10th (~1×10^{13} vg/kg

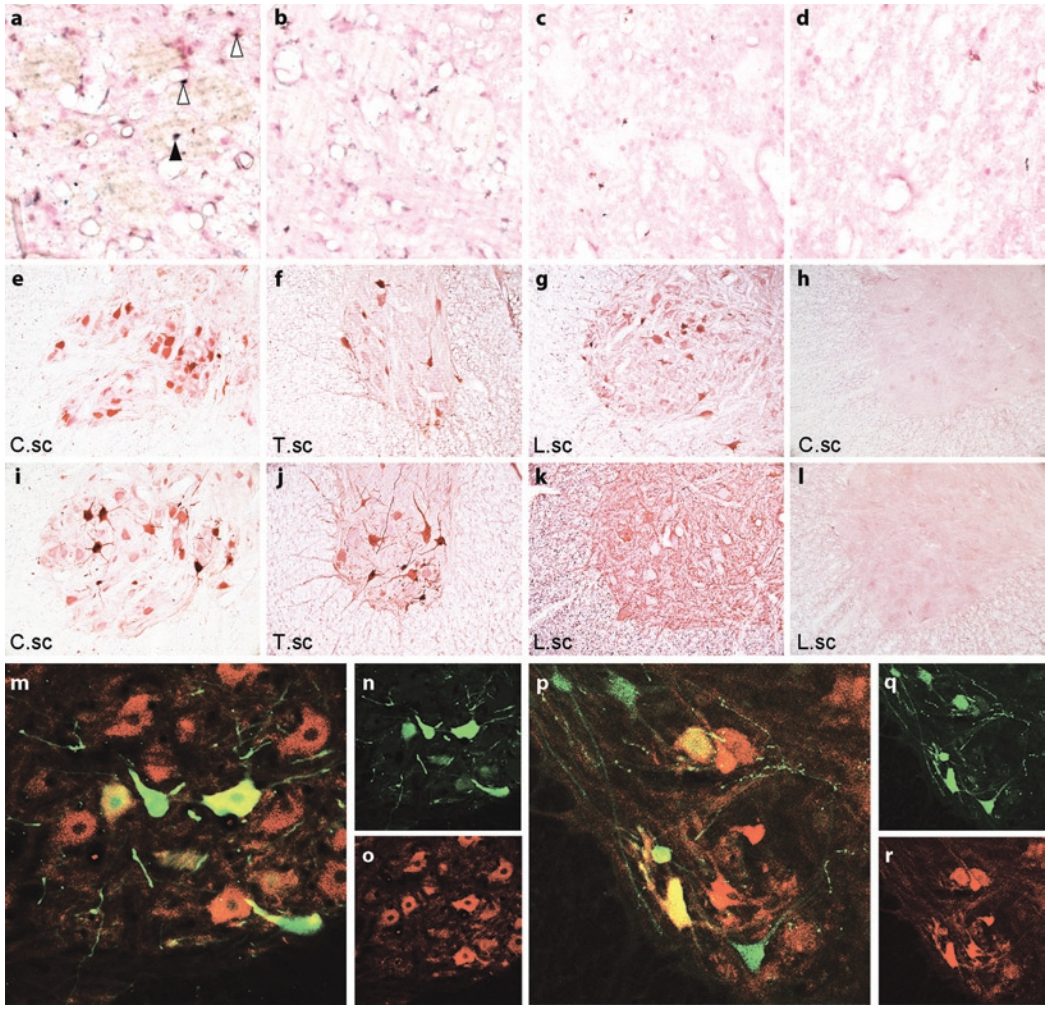

Figure 6 Pig spinal cord after adeno-associated virus type 9 (AAV9) injection. *In situ* hybridization of AAV9 (**a**–**b**) or phosphate-buffered saline (PBS) (**c**–**d**)-injected spinal cords reveals green fluorescent protein (GFP) signal within motor neurons (filled arrows) and glia (open arrows) of antisense probed sections of (**a**) AAV-injected pigs but not (**c**) PBS injected. Sense probed sections from both treated and control animals had no detectable signal (**b** and **d**). Immunohistochemical detection of GFP following (**e**–**h**) intracisternal or (**i**–**l**) intrathecal-injected spinal cords indicates extensive labeling of large ventral horn neurons within AAV9-injected (**e**–**g** and **i**–**k**) but not PBS-injected animals (**h** and **l**). Immunofluorescent colabeling of GFP (**n** and **q**) and ChAT (**o** and **r**) in spinal cord sections from intracisternal or intrathecal AAV9-injected pigs shows that the transduced cells are motor neurons (merged, **m** and **p**). C.sc, cervical spinal cord, T.sc, thoracic spinal cord; L.sc, lumbar spinal cord.

versus ~1 × 10^{14} vg/kg) the dose used in the present study for the P1–P90 animals and comparable to our 3-year-old animal (2.7 × 10^{13} vg/kg). The overlap in the 3-year-old age group between the two studies calls into question whether the interventional radiological techniques employed in the present study conferred an advantage with respect to first-pass CNS transduction. The occlusion of blood flow to the liver may be beneficial in improving transduction to other tissues, however, further studies are needed to assess the efficacy of procedurally detargeting the liver. Furthermore, emerging techniques in capsid evolution for enhancements of vectors have also shown effectiveness in detargeting the liver[26] and requires additional study for systemic gene delivery to the brain. Nonetheless, together the data suggest that CNS targeting following systemic injection of AAV9 is feasible in animals from birth through 4 years of age over a range of doses. A noteworthy finding between the two studies is the consistent targeting of motor neurons in all of the animals examined regardless of age. These findings will certainly have impact on the development of gene delivery protocols for SMA. Whereas type 1 SMA patients are the most severe and most common, a significant patient population exists with type 2 and type 3 disease that manifests later in life and produces milder though still debilitating symptoms.[27] The field's knowledge of the molecular pathology of mild SMA is hampered by the fact that lifespan is often not affected in these patients and a robust animal model is not available for study.[28] The preclinical SMN gene delivery studies were performed in a mouse model that closely resembles type 1 patients and therefore supports a trial within those patients.[2–4] However, because gene delivery to motor neurons can be accomplished at later time points in higher species, it gives hope for later trials in less severe patients. An important question remains though, as to whether type 2 and type 3 patients would benefit from SMN gene restoration within motor neurons at their stage of disease. Outside of motor neurons, the fact that lower doses in larger animals produced appreciable

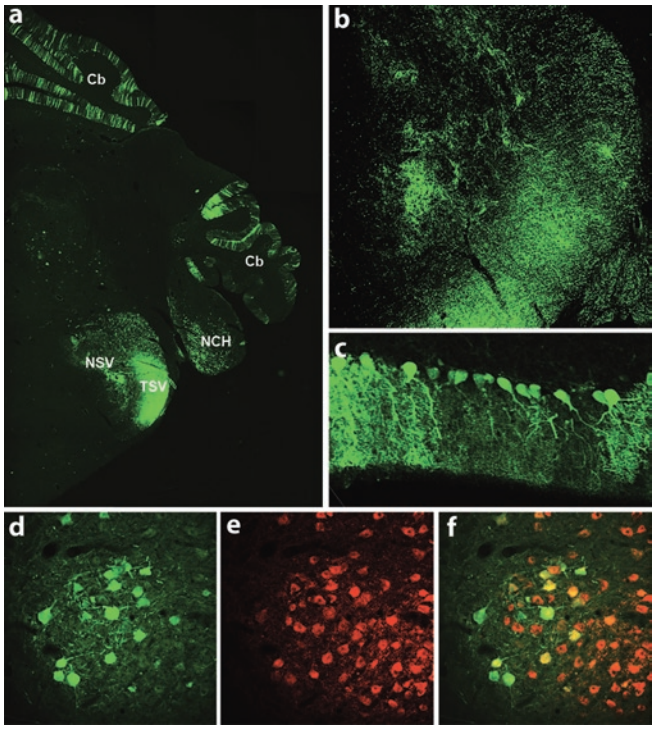

Figure 7 Adeno-associated virus type 9 (AAV9)-green fluorescent protein (GFP) mediates transgene expression in the brain after intrathecal delivery. Representative coronal brain section (a) showing GFP expression after intrathecal injection of AAV9-GFP within the hindbrain, fibers of the trigeminal nerve (b) and Purkinje cells (c). (d–f) GFP expression was also detected in ChAT$^+$ neuron of the olivary nucleus. Cb, cerebellum; NCH, nuclei cochleares; NSV, nucleus tractus spinalis nervi trigemini; TSV, tractus spinalis nervi trigemini.

transgene expression within the CNS supports the development of therapies for diseases with secreted transgenes such as lysosomal storage disorders.[29]

The studies by Gray *et al*. in 3–4-year-old Nonhuman primates show that poor expression was seen in the presence of pre-existing antibodies following systemic delivery.[12] In human clinical trials, transgene expression can be achieved following direct injection into muscle or brain despite pre-existing neutralizing antibodies.[30,31] While more information is needed regarding the prevalence of neutralizing antibodies to AAV9 within the adult population, the epidemiological data suggests that the overwhelming majority of the adult population is seronegative for neutralizing antibodies against newer AAV serotypes.[32–34] For example, AAV2 is the serotype with the highest prevalence of neutralizing antibodies ranging from 20 to 60% of the population at a 1:20 dilution, and the prevalence of individuals with neutralizing antibodies to emerging serotypes such as AAV8 was among the lowest tested (19–32% at a 1:20 dilution) across multiple continents.[33] Of interest, in a French adult population <50% of individuals from 25 to 64 years old were seropositive for AAV9-binding antibodies, of which only ~33% inhibited *in vitro* infection. Among those seropositive for anti-AAV9 antibodies, ~70% had very low antibody titers of 1:20 which was the lowest dilution tested.[32] Studies in children report that the prevalence of anti-AAV antibodies in children is less than that of adults, indicating the age of acquisition of infection may also factor favorably into delivery into a pediatric population.[35,36] It is also possible to transiently reduce or eliminate neutralizing antibodies via apheresis which may allow gene targeting even in seropositive patients.[37]

An important goal of this study was to address the existence of a window of opportunity for motor neuron targeting in nonhuman primates. In mice, systemic injection of AAV9 into older animals (P10 and older) led to a dramatic increase in the number of glia targeted within the spinal gray matter when compared to P1-injected mice.[11] Concomitant with the increase in glial targeting was a decrease in motor neuron targeting which could complicate patient selection in a clinical trial for SMA.[3,11] The successful transduction of motor neurons in all the treated monkeys suggests that the hypothetical window closes much later, if at all, in nonhuman primates. The data from both the spinal cord *in situ* hybridization and the monkey brain histology demonstrate glial cells are well transduced by AAV9 at all ages studied, suggesting that astrocytes may still be a viable target for AAV9 delivery under appropriate circumstances.

Another departure from the data generated in mice is the types of cells targeted in the brains of monkeys after systemic AAV9 injection. Experiments in mice targeted predominantly neurons throughout the brains of neonate-injected animals, whereas in monkeys the cells targeted were mostly astrocytes and microglia. This discrepancy is likely due to the different timing of gliogenesis between the two species.[38] Therefore, vector escaping from the vasculature in the primate brain would likely encounter glial endfeet that ensheathe the endothelial cells before meeting neurons. Nonetheless, the number of neurological diseases that have implicated glial cells as contributing to pathology continues to grow.[39] The abundance and distribution of cells targeted throughout the primate brains of all the treated animals suggests AAV9 gene delivery could have immense impact on diseases throughout the nervous system, such as amyotrophic lateral sclerosis, Rett syndrome, and lysosomal storage diseases.[29,40,41]

The high amount of GFP expression throughout all the skeletal muscles examined is consistent with data from numerous groups in mice and dogs.[18,22] Head-to-head comparisons would be required in nonhuman primates to determine whether the hierarchy of muscle transducing serotypes from mice is consistent in monkeys. Transduction of peripheral organs is an expected side effect of systemic delivery. Indeed, the persistence of expression in the liver of the younger primates is noteworthy when compared to data in mice in which episomal viral genomes are lost through the rapid cell divisions of the developing mouse liver. However, the slower development of primates compared to rodents likely explains why we saw GFP persistence in the liver at the time of sacrifice; 3 weeks postinjection. For example, in the P1 animal there was a difference of only 4 g between birth and sacrifice 3 weeks later. Similar vector doses in P1 mice also show the clearance of transgene expression from liver as a factor of time post injection (data not shown). Therefore, we predict the expression of transgene in nonhuman primate liver would diminish over time, due to hepatocyte division. Depending on the paradigm, transduction of organs can be potentially beneficial or harmful, and techniques exist to restrict the viral expression to target cells such as motor neurons if needed.[42–45] As for the tissues targeted in this study, our data is in agreement with data generated in cats

that showed skeletal muscle, liver and adrenal medulla as highly transduced sites following systemic injection of AAV9.[10]

Anticipating the potential requirement to avoid off-target expression of corrective transgenes outside the CNS, we have also demonstrated that AAV9 delivery into the CSF can deliver transgene throughout the CNS with limited peripheral expression. Recent studies utilizing gene transfer for SMA into the lateral ventricles and lumbar spinal cord of neonatal SMA mice had a profound effect on survival, though it is not clear how favorably it compares with systemic administration.[24,25] Development of an intrathecal delivery paradigm would reduce viral load that in turn could reduce the risk of an immune response as well as decrease viral production requirements particularly for older, presumably larger patients. Another complicating factor, at least in the context of SMA, is the involvement of non-neuronal tissues. Our group and others recently reported cardiac deficits in multiple SMA mouse models that could suggest the need for SMN protein in cells besides motor neurons.[46–48] The relevance of similar heart findings in humans also remains to be elucidated. Designing studies to examine the contribution of cell types other than motor neurons to SMA pathology is difficult due to the models available due in part to early pathology and the small size of SMA mice.

The data presented here give increasing confidence that systemic and intrathecal delivery of AAV9 will likely be successful when applied to pediatric neurological disease, potentially even in older children. The published preclinical efficacy data in a model of SMA and the effectiveness of motor neuron targeting within large animals in the current report highlight the need for safety studies utilizing SMN as the next step in advancing SMA gene delivery to clinical trial. The demonstration of motor neuron and glial targeting in large species opens the possibilities to the creation of large animal models of disease to address questions of subcellular localization of proteins or the importance of aging to the manifestation of a disease phenotype. The repertoire of AAV9 and emerging serotypes are just beginning to be explored, yet is demonstrating significant potential in basic and translational science.[49]

MATERIALS AND METHODS

Viral production. Self-complementary AAV9 was produced by transient transfection procedures using a double-stranded AAV2-ITR-based CB-GFP vector, with a plasmid encoding Rep2Cap9 sequence as previously described along with an adenoviral helper plasmid pHelper (Stratagene, Santa Clara, CA) in 293 cells.[50] Our serotype 9 sequence was verified by sequencing and was identical to that previously described. Virus was produced in three separate batches for the experiments and purified by two cesium chloride density gradient purification steps, dialyzed against PBS and formulated with 0.001% Pluronic-F68 to prevent virus aggregation and stored at 4 °C. All vector preparations were titered by quantitative-PCR using Taq-Man technology. Purity of vectors was assessed by 4–12% sodium dodecyl sulfate-acrylamide gel electrophoresis and silver staining (Invitrogen, Carlsbad, CA).

Animal care and use. All procedures performed were in accordance to either the Mannheimer Foundation (Homestead, FL), the Research Institute at Nationwide Children's Hospital or The Ohio State University Institutional Animal Care and Use Committees.

Nonhuman primate intravascular vector delivery. The breeding, housing and procedures performed on the young, male cynomolgus macaques (*Macaca fasciculata*, age P1–P90) were carried out at the Mannheimer Foundation. Briefly, veterinary staff anesthetized the subject and placed a catheter into the saphenous vein, through which either a suspension of 1–3 × 10^{14} vg/kg AAV9.CBA.GFP or PBS was infused over a period of 5–8 minutes. Upon recovery, subjects were returned to their mother and housed under routine conditions for the duration of the study.

At Nationwide Children's Hospital, the 3-year-old subject was infused with 2.7 × 10^{13} vg/kg using interventional radiological techniques to target delivery to the radicular arteries of the thoracic cord. Briefly, the subject was anesthetized and a catheter was introduced percutaneously into the brachial artery and guided to the proximal portion of the descending aorta. A second catheter delivered an occlusive balloon to the distal portion of the descending aorta at the level of the celiac trunk. Proper placement was confirmed by fluoroscopy and injection of a radiopaque dye via the proximal catheter. Before injection, the distal balloon was inflated to occlude blood flow distal to and including the celiac trunk. The viral suspension was delivered over ~1 minute, and the balloon was left inflated for another 2 minutes postinfusion. After recovery, the animal was released back to its regular environment for the duration of the study.

Seronegativity for anti-AAV9 antibodies was confirmed in all subjects by enzyme-linked immunosorbent assay. Briefly, a 2 × 10^{10} vg/ml solution of empty AAV9 capsids was made with a carbonate coating buffer and applied to a 96-well plate and incubated over night at 4 °C. The following day, the plate was washed and blocked with a 5% milk solution in PBS with 0.1% Tween-20. Serums were diluted from 1:50 to 1:6400 and incubated at room temperature for an hour. The wells were washed with PBS-T and then incubated with an horseradish peroxidase conjugated anti-monkey secondary (Sigma-Aldrich, St Louis, MO) for 1 hour at room temperature. The wells were washed with PBS-T then developed with TMB. The reaction was stopped with the addition of hydrochloric acid and absorbance was read at 650 nm on a plate reader.

Intrathecal Injection. Farm-bred sows (*Sus scrofa domestica*) were obtained from a regional farm. Five-day-old (P5) piglets received 0.5 cc/kg ketamine induction anesthesia and then were maintained by mask inhalation of 5% isoflurane in oxygen. Body temperature, electrocardiogram, and respiratory rate were monitored throughout the procedure. For lumbar puncture, piglets were placed prone and the spine was flexed in order to widen the intervertebral spaces. The anterior–superior iliac spines were palpated and a line connecting the two points was visualized. The intervertebral space rostral to this line is ~L5–L6. Intraoperative fluoroscopy confirmed rostral-caudal and mediolateral trajectories. Using sterile technique, a 25-gauge needle attached to a 1-ml syringe was inserted. Gentle negative pressure was applied to the syringe as the needle was passed until a clear flash of CSF was visualized. For cisterna puncture, the head of the piglet was flexed while maintaining the integrity of the airway. Fluoroscopy again confirmed adequate trajectory. A 25-gauge needle was passed immediately caudal to the occipital bone, and a flash of clear CSF confirmed entry into the cistern magna.

For reagent delivery, the syringe was removed while the needle was held in place. A second 1-cc syringe containing either viral solution (5.2 × 10^{12} vg/kg) or PBS was secured and the solution was injected into the intrathecal space at a slow and constant rate. After delivery, ~0.25 ml of sterile PBS was flushed through the spinal needle so as to ensure full delivery of reagent.

We confirmed rostral and caudal intrathecal flow by injecting a radioopaque agent (Omnipaque, GE Healthcare, Waukesha, WI) and recording intrathecal spread with real-time continuous fluoroscopy.

Perfusion and tissue-processing. All subjects (primate and porcine) were killed between 21 and 24 days postinjection. Subjects were deeply anesthetized by intramuscular injection of sodium pentobarbital solution (primates) or Telazol followed by Propofol (piglets). A midventral sternal thoracotomy was performed and a cannula was inserted in the aorta through the left ventricle. The right atrium was opened and 0.5–1 l of PBS

was injected through the cannula by gravity flow, followed by perfusion with 1 l of 4% paraformaldehyde in phosphate buffer (pH 7.4). Organs were removed and post-fixed 48 hours in 4% paraformaldehyde before further processing for histological sectioning or stored long-term in 0.1% NaN_3 PBS solution.

Histology and microscopy. Primate and porcine spinal cord segments were embedded in 3% agarose before cutting into 40-µm horizontal sections using a Leica VT1200 vibrating microtome (Leica Microsystems, Buffalo Grove, IL). Sections were transferred in Tris-buffered saline and stored at 4 °C until processing.

Primate and porcine brains were cryoprotected by successive incubation in 10, 20, and 30% sucrose solutions. Once sufficiently cryoprotected (having sunk in 30% sucrose solution), brains were frozen and whole-mounted on a modified Leica SM 2000R sliding microtome (Leica Microsystems) in OCT (Tissue-Tek, Torrance, CA) and cut into 40-µm coronal sections.

For immunofluorescent determination of cell types transduced, floating sections were submerged in blocking solution (10% donkey serum, 1% Triton-X100 in Tris-buffered saline) for 1 hour followed by overnight incubation in primary antibody solution at 4 °C. The following primary antibodies were used in this study: Rabbit-anti-GFP (1:500; Invitrogen), goat-anti-ChAT (1:100; Millipore, Billerica, MA), guinea-pig-anti-GFAP (1:1,000; Advanced Immunochemical, Long Beach, CA) and rabbit-anti-Iba1 (1:500; Dako, Carpentaria, CA). Primary antibodies were detected using Fitc-, Cy3-, or Cy5-conjugated secondary antibodies (1:1,000; Jackson ImmunoResearch, West Grove, PA) and mounted in PVA-DABCO medium.

For immunohistochemical staining, sections were incubated at room temperature in 0.5% H_2O_2/10% MeOH solution and subsequently blocked and stained as above with rabbit-anti-GFP overnight. Anti-GFP antibodies were detected using biotinylated donkey-anti-rabbit secondary antibody (1:200; Jackson ImmunoResearch) and developed using Vector NovaRed per the provided protocol (Vector Labs, Burlingame, CA). Sections were then mounted in Cytoseal 60 medium (Thermo Fisher Scientific, Kalamazoo, MI).

Non-neural tissues were cut to ~1 cm^3 blocks and cryoprotected by overnight incubation in 30% sucrose solution. They were then embedded in gum tragacanth and flash-frozen in liquid nitrogen-cooled isopentane. Samples were cut by cryostat into 10–12 µm sections and slides stored at −20 °C. GFP expression was detected by a similar immunofluorescent protocol as above with the addition of DAPI in secondary antibody solution (1:1,000; Invitrogen).

Fluorescent images were captured using a Zeiss 710 Meta confocal microscope (Carl Zeiss MicroImaging, Thornwood, NY) located at TRINCH and processed with LSM software.

Whole brain sections were scanned to ×40 resolution at the Biopathology Center in the Research Informatics Core at the Research Institute at Nationwide Children's Hospital using an Aperio automated slide scanner (Aperio, Vista, CA) and resulting images were processed with ImageScope software.

In situ *hybridization.* As described previously,[11] we generated antisense and sense DIG-UTP-labeled GFP riboprobes. Probe yield and incorporation of DIG-UTP was confirmed by electrophoresis and dot blot. Sections of spinal cord 10-µm thick were mounted and prepared by fixation with 4% paraformaldehyde, washed in 0.5× SSC, permeabilized by incubation in proteinase K (2.5 µg/ml), washed in 0.5 × SSC and dehydrated in series of alcohol washes. Prehybridization was performed at 42 °C using RiboHybe buffer (Ventana, Tucson, AZ) for 1 hour followed by hybridization overnight at 55 °C with the respective riboprobes on AAV9-injected and PBS-control-injected cord sections. Stringency washes were performed and immunological detection using anti-Digoxigenin AP antibody (1:500; Roche, Tucson, AZ) and development with NBT/BCIP (Thermo Fisher Scientific) and Nuclear Fast Red (Vector Labs).

SUPPLEMENTARY MATERIAL

Figure S1. GFP expression with the dorsal horn of spinal cord.
Figure S2. GFP expression in a 3-year-old monkey spinal cord.
Figure S3. GFP immunohistochemistry from a 3-year-old monkey.
Figure S4. GFP immunofluorescence from AAV9-injected monkey brain.

ACKNOWLEDGMENTS

This work was supported by NIH RC2 NS69476-01 (to A.H.M.B. and B.K.K.) and Families of SMA (to B.K.K.) A.K.B., S.D., K.D.F., A.H.M.B., and B.K.K. designed and executed the experiments. K.D.F., A.K.B., and B.K.K. wrote the manuscript. P.R.M. performed the young primate experiments. L.B. and L.S. contributed to histological analysis. C.M.C. performed the *in situ* hybridization. M.M., L.G.C., and B.D.C. performed the interventional radiology. S.D., P.N.P., and S.J.K. performed the pig experiments. Our thanks to Tom Barr and Stephanie Weaver of the Biopathology Center in the Research Informatics Core at the Research Institute at Nationwide Children's Hospital for slide scanning.

REFERENCES

1. Kolb, SJ and Kissel, JT (2011). Spinal muscular atrophy: A timely review. *Arch Neurol* (epub ahead of print).
2. Dominguez, E, Marais, T, Chatauret, N, Benkhelifa-Ziyyat, S, Duque, S, Ravassard, P *et al.* (2011). Intravenous scAAV9 delivery of a codon-optimized SMN1 sequence rescues SMA mice. *Hum Mol Genet* **20**: 681–693.
3. Foust, KD, Wang, X, McGovern, VL, Braun, L, Bevan, AK, Haidet, AM *et al.* (2010). Rescue of the spinal muscular atrophy phenotype in a mouse model by early postnatal delivery of SMN. *Nat Biotechnol* **28**: 271–274.
4. Valori, CF, Ning, K, Wyles, M, Mead, RJ, Grierson, AJ, Shaw, PJ *et al.* (2010). Systemic delivery of scAAV9 expressing SMN prolongs survival in a model of spinal muscular atrophy. *Sci Transl Med* **2**: 35ra42.
5. Anderton, RS, Meloni, BP, Mastaglia, FL, Greene, WK and Boulos, S (2011). Survival of motor neuron protein over-expression prevents calpain-mediated cleavage and activation of procaspase-3 in differentiated human SH-SY5Y cells. *Neuroscience* **181**: 226–233.
6. La Bella, V, Kallenbach, S and Pettmann, B (2000). Expression and subcellular localization of two isoforms of the survival motor neuron protein in different cell types. *J Neurosci Res* **62**: 346–356.
7. Vitte, JM, Davoult, B, Roblot, N, Mayer, M, Joshi, V, Courageot, S *et al.* (2004). Deletion of murine Smn exon 7 directed to liver leads to severe defect of liver development associated with iron overload. *Am J Pathol* **165**: 1731–1741.
8. Zhang, Z, Lotti, F, Dittmar, K, Younis, I, Wan, L, Kasim, M *et al.* (2008). SMN deficiency causes tissue-specific perturbations in the repertoire of snRNAs and widespread defects in splicing. *Cell* **133**: 585–600.
9. Burghes, AH and Beattie, CE (2009). Spinal muscular atrophy: why do low levels of survival motor neuron protein make motor neurons sick? *Nat Rev Neurosci* **10**: 597–609.
10. Duque, S, Joussemet, B, Riviere, C, Marais, T, Dubreil, L, Douar, AM *et al.* (2009). Intravenous administration of self-complementary AAV9 enables transgene delivery to adult motor neurons. *Mol Ther* **17**: 1187–1196.
11. Foust, KD, Nurre, E, Montgomery, CL, Hernandez, A, Chan, CM and Kaspar, BK (2009). Intravascular AAV9 preferentially targets neonatal neurons and adult astrocytes. *Nat Biotechnol* **27**: 59–65.
12. Gray, SJ, Matagne, V, Bachaboina, L, Yadav, S, Ojeda, SR and Samulski, RJ (2011). Preclinical Differences of Intravascular AAV9 Delivery to Neurons and Glia: A Comparative Study of Adult Mice and Nonhuman Primates. *Mol Ther* **19**: 1058–1069.
13. Wang, DB, Dayton, RD, Henning, PP, Cain, CD, Zhao, LR, Schrott, LM *et al.* (2010). Expansive gene transfer in the rat CNS rapidly produces amyotrophic lateral sclerosis relevant sequelae when TDP-43 is overexpressed. *Mol Ther* **18**: 2064–2074.
14. Alvarez-Saavedra, M, Carrasco, L, Sura-Trueba, S, Demarchi Aiello, V, Walz, K, Neto, JX *et al.* (2010). Elevated expression of MeCP2 in cardiac and skeletal tissues is detrimental for normal development. *Hum Mol Genet* **19**: 2177–2190.
15. Forsayeth, JR and Bankiewicz, KS (2011). AAV9: Over the Fence and Into the Woods. *Mol Ther* **19**: 1006–1007.
16. Daniel, C, Rojo, MG, Klossa, J, Mea, VD, Booker, D, Beckwith, BA *et al.* (2011). Standardizing the use of whole slide images in digital pathology. *Comput Med Imaging Graph*.
17. Kota, J, Handy, CR, Haidet, AM, Montgomery, CL, Eagle, A, Rodino-Klapac, LR *et al.* (2009). Follistatin gene delivery enhances muscle growth and strength in nonhuman primates. *Sci Transl Med* **1**: 6ra15.
18. Bish, LT, Morine, K, Sleeper, MM, Sanmiguel, J, Wu, D, Gao, G *et al.* (2008). Adeno-associated virus (AAV) serotype 9 provides global cardiac gene transfer superior to AAV1, AAV6, AAV7, and AAV8 in the mouse and rat. *Hum Gene Ther* **19**: 1359–1368.
19. Kornegay, JN, Li, J, Bogan, JR, Bogan, DJ, Chen, C, Zheng, H *et al.* (2010). Widespread muscle expression of an AAV9 human mini-dystrophin vector after intravenous injection in neonatal dystrophin-deficient dogs. *Mol Ther* **18**: 1501–1508.
20. Pacak, CA, Sakai, Y, Thattaliyath, BD, Mah, CS and Byrne, BJ (2008). Tissue specific promoters improve specificity of AAV9 mediated transgene expression following intravascular gene delivery in neonatal mice. *Genet Vaccines Ther* **6**: 13.
21. Zincarelli, C, Soltys, S, Rengo, G and Rabinowitz, JE (2008). Analysis of AAV serotypes 1-9 mediated gene expression and tropism in mice after systemic injection. *Mol Ther* **16**: 1073–1080.

22. Yue, Y, Ghosh, A, Long, C, Bostick, B, Smith, BF, Kornegay, JN *et al.* (2008). A single intravenous injection of adeno-associated virus serotype-9 leads to whole body skeletal muscle transduction in dogs. *Mol Ther* **16**: 1944–1952.
23. Gavrilina, TO, McGovern, VL, Workman, E, Crawford, TO, Gogliotti, RG, DiDonato, CJ *et al.* (2008). Neuronal SMN expression corrects spinal muscular atrophy in severe SMA mice while muscle-specific SMN expression has no phenotypic effect. *Hum Mol Genet* **17**: 1063–1075.
24. Passini, MA, Bu, J, Richards, AM, Kinnecom, C, Sardi, SP, Stanek, LM *et al.* (2011). Antisense oligonucleotides delivered to the mouse CNS ameliorate symptoms of severe spinal muscular atrophy. *Sci Transl Med* **3**: 72ra18.
25. Passini, MA, Bu, J, Roskelley, EM, Richards, AM, Sardi, SP, O'Riordan, CR *et al.* (2010). CNS-targeted gene therapy improves survival and motor function in a mouse model of spinal muscular atrophy. *J Clin Invest* **120**: 1253–1264.
26. Pulicherla, N, Shen, S, Yadav, S, Debbink, K, Govindasamy, L, Agbandje-McKenna, M *et al.* (2011). Engineering Liver-detargeted AAV9 Vectors for Cardiac and Musculoskeletal Gene Transfer. *Mol Ther* **19**: 1070–1078.
27. Zerres, K, Rudnik-Schöneborn, S, Forrest, E, Lusakowska, A, Borkowska, J and Hausmanowa-Petrusewicz, I (1997). A collaborative study on the natural history of childhood and juvenile onset proximal spinal muscular atrophy (type II and III SMA): 569 patients. *J Neurol Sci* **146**: 67–72.
28. Park, GH, Kariya, S and Monani, UR (2010). Spinal muscular atrophy: new and emerging insights from model mice. *Curr Neurol Neurosci Rep* **10**: 108–117.
29. Fu, H, Dirosario, J, Killedar, S, Zaraspe, K and McCarty, DM (2011). Correction of Neurological Disease of Mucopolysaccharidosis IIIB in Adult Mice by rAAV9 Trans-Blood-Brain Barrier Gene Delivery. *Mol Ther* **19**: 1025–1033.
30. Brantly, ML, Chulay, JD, Wang, L, Mueller, C, Humphries, M, Spencer, LT *et al.* (2009). Sustained transgene expression despite T lymphocyte responses in a clinical trial of rAAV1-AAT gene therapy. *Proc Natl Acad Sci USA* **106**: 16363–16368.
31. Kaplitt, MG, Feigin, A, Tang, C, Fitzsimons, HL, Mattis, P, Lawlor, PA *et al.* (2007). Safety and tolerability of gene therapy with an adeno-associated virus (AAV) borne GAD gene for Parkinson's disease: an open label, phase I trial. *Lancet* **369**: 2097–2105.
32. Boutin, S, Monteilhet, V, Veron, P, Leborgne, C, Benveniste, O, Montus, MF *et al.* (2010). Prevalence of serum IgG and neutralizing factors against adeno-associated virus (AAV) types 1, 2, 5, 6, 8, and 9 in the healthy population: implications for gene therapy using AAV vectors. *Hum Gene Ther* **21**: 704–712.
33. Calcedo, R, Vandenberghe, LH, Gao, G, Lin, J and Wilson, JM (2009). Worldwide epidemiology of neutralizing antibodies to adeno-associated viruses. *J Infect Dis* **199**: 381–390.
34. van der Marel, S, Comijn, EM, Verspaget, HW, van Deventer, S, van den Brink, GR, Petry, H *et al.* (2011). Neutralizing antibodies against adeno-associated viruses in inflammatory bowel disease patients: Implications for gene therapy. *Inflamm Bowel Dis* (epub ahead of print).
35. Chen, CL, Jensen, RL, Schnepp, BC, Connell, MJ, Shell, R, Sferra, TJ *et al.* (2005). Molecular characterization of adeno-associated viruses infecting children. *J Virol* **79**: 14781–14792.
36. Erles, K, Sebökovà, P and Schlehofer, JR (1999). Update on the prevalence of serum antibodies (IgG and IgM) to adeno-associated virus (AAV). *J Med Virol* **59**: 406–411.
37. Tydén, G, Kumlien, G and Efvergren, M (2007). Present techniques for antibody removal. *Transplantation* **84**(12 Suppl): S27–S29.
38. Caley, DW and Maxwell, DS (1970). Development of the blood vessels and extracellular spaces during postnatal maturation of rat cerebral cortex. *J Comp Neurol* **138**: 31–47.
39. Amor, S, Puentes, F, Baker, D and van der Valk, P (2010). Inflammation in neurodegenerative diseases. *Immunology* **129**: 154–169.
40. Ballas, N, Lioy, DT, Grunseich, C and Mandel, G (2009). Non-cell autonomous influence of MeCP2-deficient glia on neuronal dendritic morphology. *Nat Neurosci* **12**: 311–317.
41. Ilieva, H, Polymenidou, M and Cleveland, DW (2009). Non-cell autonomous toxicity in neurodegenerative disorders: ALS and beyond. *J Cell Biol* **187**: 761–772.
42. Xie, J, Xie, Q, Zhang, H, Ameres, SL, Hung, JH, Su, Q *et al.* (2011). MicroRNA-regulated, systemically delivered rAAV9: a step closer to CNS-restricted transgene expression. *Mol Ther* **19**: 526–535.
43. Gray, SJ, Blake, BL, Criswell, HE, Nicolson, SC, Samulski, RJ, McCown, TJ *et al.* (2010). Directed evolution of a novel adeno-associated virus (AAV) vector that crosses the seizure-compromised blood-brain barrier (BBB). *Mol Ther* **18**: 570–578.
44. Jang, JH, Schaffer, DV and Shea, LD (2011). Engineering biomaterial systems to enhance viral vector gene delivery. *Mol Ther* (epub ahead of print).
45. Hester, ME, Murtha, MJ, Song, S, Rao, M, Miranda, CJ, Meyer, K *et al.* Rapid and efficient generation of functional motor neurons from human pluripotent stem cells using gene delivered transcription factor codes. *Mol Ther* (epub ahead of print).
46. Bevan, AK, Hutchinson, KR, Foust, KD, Braun, L, McGovern, VL, Schmelzer, L *et al.* (2010). Early heart failure in the SMNDelta7 model of spinal muscular atrophy and correction by postnatal scAAV9-SMN delivery. *Hum Mol Genet* **19**: 3895–3905.
47. Heier, CR, Satta, R, Lutz, C and DiDonato, CJ (2010). Arrhythmia and cardiac defects are a feature of spinal muscular atrophy model mice. *Hum Mol Genet* **19**: 3906–3918.
48. Shababi, M, Habibi, J, Yang, HT, Vale, SM, Sewell, WA and Lorson, CL (2010). Cardiac defects contribute to the pathology of spinal muscular atrophy models. *Hum Mol Genet* **19**: 4059–4071.
49. Zhang, H, Yang, B, Mu, X, Ahmed, SS, Su, Q, He, R *et al.* Several rAAV vectors efficiently cross the blood-brain barrier and transduce neurons and astrocytes in the neonatal mouse central nervous system. *Mol Ther* (epub ahead of print).
50. Gao, G, Vandenberghe, LH, Alvira, MR, Lu, Y, Calcedo, R, Zhou, X *et al.* (2004). Clades of Adeno-associated viruses are widely disseminated in human tissues. *J Virol* **78**: 6381–6388.